

# Observing Application

Date: Aug 03, 2020
Proposal ID: VLA/21A-203
Legacy ID: AR1055
PI: Michael Rugel
Type: Regular
Category: Interstellar Medium
Total time: 34.8

## HI and OH observations to complement SOFIA HyGAL legacy program

### Abstract:

Our understanding of the diffuse interstellar medium has greatly improved with absorption line spectroscopy of atoms and small molecules, though only the brightest and most well-studied sources have been investigated. To extend these successful efforts to a greater variety of sources, we are carrying out a Joint (i.e. US - German) SOFIA Legacy Program, "HyGAL" over the next two years. This 82-hour program, which was approved in full last December, will conduct absorption line observations of six hydride molecules. Previous JVLA absorption-line observations of the 21 cm HI line (Winkel et al. 2017), have proven essential to the interpretation of many of these molecular line data obtained at shorter wavelengths. To fully exploit the data to be obtained in HyGAL, HI observations are essential. Also, for an understanding of the OH 18 cm line intensities, which usually are not in thermal equilibrium, the combination of JVLA and SOFIA data will provide a critical calibration of the 18 cm lines. To obtain high-sensitivity observations of the HI and OH transitions, we request 34.8h of telescope time for L-band observations in C-configuration. In addition to the HI and OH data we shall also obtain radio continuum and recombination line data.

### Authors:

Name	Institution	Email	Status
Neufeld, David	Johns Hopkins University	neufeld@pha.jhu.edu	
Menten, Karl	Max-Planck-Institut für Radioastronomie	kmenten@mpifr-bonn.mpg.de	
Jacob, Arshia	Max-Planck-Institut für Radioastronomie	ajacob@mpifr-bonn.mpg.de	Graduating: N/A Thesis: false
Winkel, Benjamin	Max-Planck-Institut für Radioastronomie	bwinkel@mpifr.de	
Rugel, Michael	Max-Planck-Institut für Radioastronomie	mrugel@mpifr-bonn.mpg.de	
Wiesemeyer, Helmut	Max-Planck-Institut für Radioastronomie	hwiese@mpifr.de	

Principal Investigator: Michael Rugel  
Contact: Michael Rugel  
Telephone: +49 (0)228-525-171  
Email: mrugel@mpifr-bonn.mpg.de

### Related Proposals:

### Joint:

Not a Joint Proposal.

### Observing type(s):

Spectroscopy

### VLA Resources

Name	Conf.	Frontend & Backend	Setup
L-band commensality	C	L Band 20 cm 1000 - 2000 MHz General and Shared Risk Observing - Spectral Line	Rest frequencies: 1.5 GHz

### L-band commensality

GOST 20A (v1.0)

Subbands View Help This configuration is Standard

Receiver Band: L (1-2 GHz) | Center Freq (GHz): 1.5 | Center Freq (GHz): 1.5 | Dump Time (s) [defaults]: 10.0

A/C Basebands:  3-bit  8-bit | A0/C0: 1.5 | Total Data Rate [limits]: 34.5MB/s, 124.1GB/h

B/D Basebands:  3-bit  8-bit | B0/D0: 1.5 | Channels x Polarization Products Used: 9728 of 16384

Baseline Board Pairs Used: 38 of 64

SB	Velo Cov	BW	Prod	Recirc	BIBP	Ch Wd (v)	Ch Wd (f)	Channels	MB/s
0	800 km/s	4.0MHz	Dual	32	2	97.6 m/s	488 Hz	8,192	4.7
1	800 km/s	4.0MHz	Dual	8	1	781 m/s	3.91 kHz	1,024	0.59
2	800 km/s	4.0MHz	Dual	8	1	781 m/s	3.91 kHz	1,024	0.59
3	800 km/s	4.0MHz	Dual	8	1	781 m/s	3.91 kHz	1,024	0.59
4	800 km/s	4.0MHz	Dual	8	1	781 m/s	3.91 kHz	1,024	0.59
5	800 km/s	4.0MHz	Dual	8	1	781 m/s	3.91 kHz	1,024	0.59
6	800 km/s	4.0MHz	Dual	8	1	781 m/s	3.91 kHz	1,024	0.59
7	800 km/s	4.0MHz	Dual	8	1	781 m/s	3.91 kHz	1,024	0.59
8	800 km/s	4.0MHz	Dual	8	1	781 m/s	3.91 kHz	1,024	0.59
9	800 km/s	4.0MHz	Dual	8	1	781 m/s	3.91 kHz	1,024	0.59
10	800 km/s	4.0MHz	Dual	8	1	781 m/s	3.91 kHz	1,024	0.59
11	26000 km/s	128.0MHz	Full	1	1	400 km/s	2.00 MHz	64	0....
12	26000 km/s	128.0MHz	Full	1	1	400 km/s	2.00 MHz	64	0....
13	26000 km/s	128.0MHz	Full	1	1	400 km/s	2.00 MHz	64	0....

SB	Velo Cov	BW	Prod	Recirc	BIBP	Ch Wd (v)	Ch Wd (f)	Channels	MB/s
0	800 km/s	4.0MHz	Dual	32	2	97.6 m/s	488 Hz	8,192	4.7
1	1600 km/s	8.0MHz	Dual	16	8	97.6 m/s	488 Hz	16,384	9.4
2	800 km/s	4.0MHz	Dual	32	2	97.6 m/s	488 Hz	8,192	4.7
3	800 km/s	4.0MHz	Dual	8	1	781 m/s	3.91 kHz	1,024	0.59
4	800 km/s	4.0MHz	Dual	8	1	781 m/s	3.91 kHz	1,024	0.59
5	800 km/s	4.0MHz	Dual	8	1	781 m/s	3.91 kHz	1,024	0.59
6	800 km/s	4.0MHz	Dual	8	1	781 m/s	3.91 kHz	1,024	0.59
7	800 km/s	4.0MHz	Dual	8	1	781 m/s	3.91 kHz	1,024	0.59
8	800 km/s	4.0MHz	Dual	8	1	781 m/s	3.91 kHz	1,024	0.59
9	800 km/s	4.0MHz	Dual	8	1	781 m/s	3.91 kHz	1,024	0.59
10	800 km/s	4.0MHz	Dual	8	1	781 m/s	3.91 kHz	1,024	0.59
11	26000 km/s	128.0MHz	Full	1	1	400 km/s	2.00 MHz	64	0....
12	26000 km/s	128.0MHz	Full	1	1	400 km/s	2.00 MHz	64	0....
13	26000 km/s	128.0MHz	Full	1	1	400 km/s	2.00 MHz	64	0....

### Sources

Name	Position		Velocity		Group
NGC 6334 I	Coordinate system	Equatorial	Convention	Radio	Hygal1
	Equinox	J2000			
	Right Ascension	17:20:53.35	Ref. frame	LSRK	
		00:00:00			
	Declination	-35:47:01.5	Velocity	0.0	
00:00:00					
Calibrator	No				

Name	Position		Velocity		Group
G357.558-00.321	Coordinate system	Equatorial	Convention	Radio	Hygal1
	Equinox	J2000			
	Right Ascension	17:40:57.19	Ref. frame	LSRK	
		00:00:00			
	Declination	-31:10:59.3	Velocity	0.0	
00:00:00					
Calibrator	No				
Sgr B2M	Coordinate system	Equatorial	Convention	Radio	Hygal1
	Equinox	J2000			
	Right Ascension	17:47:20.50	Ref. frame	LSRK	
		00:00:00			
	Declination	-28:23:06.0	Velocity	0.0	
00:00:00					
Calibrator	No				
HGAL0.55-0.85	Coordinate system	Equatorial	Convention	Radio	Hygal1
	Equinox	J2000			
	Right Ascension	17:50:14.52	Ref. frame	LSRK	
		00:00:00			
	Declination	-28:54:30.7	Velocity	0.0	
00:00:00					
Calibrator	No				
G09.622+0.19	Coordinate system	Equatorial	Convention	Radio	Hygal1
	Equinox	J2000			
	Right Ascension	18:06:14.90	Ref. frame	LSRK	
		00:00:00			
	Declination	-20:31:37.0	Velocity	0.0	
00:00:00					
Calibrator	No				
G10.47+0.03	Coordinate system	Equatorial	Convention	Radio	Hygal1
	Equinox	J2000			
	Right Ascension	18:08:38.40	Ref. frame	LSRK	
		00:00:00			
	Declination	-19:51:52.0	Velocity	0.0	
00:00:00					
Calibrator	No				
G10.62-0.39	Coordinate system	Equatorial	Convention	Radio	Hygal1
	Equinox	J2000			
	Right Ascension	18:10:28.70	Ref. frame	LSRK	
		00:00:00			
	Declination	-19:55:50.0	Velocity	0.0	
00:00:00					
Calibrator	No				

Name	Position		Velocity		Group
W33A	Coordinate system	Equatorial	Convention	Radio	Hygal1
	Equinox	J2000			
	Right Ascension	18:14:39.40	Ref. frame	LSRK	
		00:00:00			
	Declination	-17:52:00.0	Velocity	0.0	
00:00:00					
Calibrator	No				
G19.61-0.23	Coordinate system	Equatorial	Convention	Radio	Hygal1
	Equinox	J2000			
	Right Ascension	18:27:38.00	Ref. frame	LSRK	
		00:00:00			
	Declination	-11:56:39.5	Velocity	0.0	
00:00:00					
Calibrator	No				
G29.96-0.02	Coordinate system	Equatorial	Convention	Radio	Hygal2
	Equinox	J2000			
	Right Ascension	18:46:03.72	Ref. frame	LSRK	
		00:00:00			
	Declination	-2:39:21.2	Velocity	0.0	
00:00:00					
Calibrator	No				
W43 MM1	Coordinate system	Equatorial	Convention	Radio	Hygal2
	Equinox	J2000			
	Right Ascension	18:47:47.00	Ref. frame	LSRK	
		00:00:00			
	Declination	-1:54:28.0	Velocity	0.0	
00:00:00					
Calibrator	No				
G31.41+0.3	Coordinate system	Equatorial	Convention	Radio	Hygal2
	Equinox	J2000			
	Right Ascension	18:47:34.10	Ref. frame	LSRK	
		00:00:00			
	Declination	-1:12:49.0	Velocity	0.0	
00:00:00					
Calibrator	No				
G32.80+0.19	Coordinate system	Equatorial	Convention	Radio	Hygal2
	Equinox	J2000			
	Right Ascension	18:50:30.62	Ref. frame	LSRK	
		00:00:00			
	Declination	-00:02:00.0	Velocity	0.0	
00:00:00					
Calibrator	No				

Name	Position		Velocity		Group
G34.3+0.2	Coordinate system	Equatorial	Convention	Radio	Hygal2
	Equinox	J2000			
	Right Ascension	18:53:18.70	Ref. frame	LSRK	
		00:00:00			
	Declination	+01:14:58.0	Velocity	0.0	
00:00:00					
Calibrator	No				
W49N	Coordinate system	Equatorial	Convention	Radio	Hygal2
	Equinox	J2000			
	Right Ascension	19:10:13.20	Ref. frame	LSRK	
		00:00:00			
	Declination	+09:06:12.0	Velocity	0.0	
00:00:00					
Calibrator	No				
G45.07+0.13	Coordinate system	Equatorial	Convention	Radio	Hygal2
	Equinox	J2000			
	Right Ascension	19:13:22.00	Ref. frame	LSRK	
		00:00:00			
	Declination	+10:50:54.0	Velocity	0.0	
00:00:00					
Calibrator	No				
W51	Coordinate system	Equatorial	Convention	Radio	Hygal2
	Equinox	J2000			
	Right Ascension	19:23:43.90	Ref. frame	LSRK	
		00:00:00			
	Declination	+14:30:31.0	Velocity	0.0	
00:00:00					
Calibrator	No				
W3 IRS 5	Coordinate system	Equatorial	Convention	Radio	Hygal3
	Equinox	J2000			
	Right Ascension	02:25:40.54	Ref. frame	LSRK	
		00:00:00			
	Declination	+62:05:51.4	Velocity	0.0	
00:00:00					
Calibrator	No				
W3(OH)	Coordinate system	Equatorial	Convention	Radio	Hygal3
	Equinox	J2000			
	Right Ascension	02:27:04.10	Ref. frame	LSRK	
		00:00:00			
	Declination	+61:52:22.1	Velocity	0.0	
00:00:00					
Calibrator	No				

Name	Position		Velocity		Group
DR21	Coordinate system	Equatorial	Convention	Radio	Hygal3
	Equinox	J2000			
	Right Ascension	20:39:01.60	Ref. frame	LSRK	
		00:00:00			
	Declination	+42:19:37.9	Velocity	0.0	
00:00:00					
Calibrator	No				
DR21(OH)	Coordinate system	Equatorial	Convention	Radio	Hygal3
	Equinox	J2000			
	Right Ascension	20:39:00.70	Ref. frame	LSRK	
		00:00:00			
	Declination	+42:22:47.0	Velocity	0.0	
00:00:00					
Calibrator	No				
NGC 7538 IRS 1	Coordinate system	Equatorial	Convention	Radio	Hygal3
	Equinox	J2000			
	Right Ascension	23:13:45.31	Ref. frame	LSRK	
		00:00:00			
	Declination	+61:28:11.7	Velocity	0.0	
00:00:00					
Calibrator	No				

**Sessions:**

Name	Session time (hours)	Repeat	Separation	LST minimum	LST maximum	Elevation minimum
Hygal Sourcegroup 1	3.3	4	0 day	14:30:00	20:00:00	10
Hygal Sourcegroup 2	3.0	4	0 day	14:30:00	23:00:00	20
Hygal Sourcegroup 3	2.4	4	0 day	19:00:00	24:00:00	20

**Session Constraints:**

Name	Scheduling constraints	Comments
Hygal Sourcegroup 1		
Hygal Sourcegroup 2		
Hygal Sourcegroup 3		

**Session Source/Resource Pairs:**

Session name	Source	Resource	Time
Hygal Sourcegroup 1	NGC 6334 I G357.558-00.321 Sgr B2M HGAL0.55-0.85 G09.622+0.19 G10.47+0.03 G10.62-0.39	L-band commensality	3.3 hour

Session name	Source	Resource	Time
	W33A G19.61-0.23		
Hygal Sourcegroup 2	G29.96-0.02 W43 MM1 G31.41+0.3 G32.80+0.19 G34.3+0.2 W49N G45.07+0.13 W51	L-band commensality	3.0 hour
Hygal Sourcegroup 3	W3 IRS 5 W3(OH) DR21 DR21(OH) NGC 7538 IRS 1	L-band commensality	2.4 hour

Present for observation: no

Staff support:

Plan of dissertation: no

## Technical Justification:

### Combined telescopes:

One of the goals of this proposal is to probe the HI content along the line of sight to Galactic continuum sources.

For HI, to determine the short-spacing correction and obtain brightness temperatures needed for spin temperature and column density determinations, we will use HI emission maps from the HI4PI survey (HI4PI collaboration 2016, A&A 594A, 116H), consisting of data from the 64 m Parkes/Australia and 100 m Effelsberg/Germany radio telescopes.

### Array configuration:

The proposed observations will be conducted in C-configuration (corresponding to  $\sim 14''$ ), which is well-matched to the SOFIA OH observations with a typical beam with of  $\sim 12''$  (see, e.g., Wiesemeyer et al. 2016, A&A, 585, 76). While our sources may be spatially extended, our main interest is the absorption towards the peak continuum source. However, C-configuration will allow us to nominally obtain resolved OH and HI absorption for sources with angular size of up to 970 arcsec.

### Subarrays:

#### Future semesters:

N/A

### Scheduling restrictions:

1. All sources rise at night, with many of the source also being visible during and after sunrise. We have no special restriction for the proposed L-band observations. All sources are outside sun avoidance.
2. The target elevation will be minimum 10-20 degree, with the majority of the observations elevations  $>20$  degree.
3. N/A
4. N/A
5. N/A

### LST Range Justification:

We set the minimum/maximum LST to the largest minimum/smallest maximum LST of all sources within each source group. In order to improve uv-coverage, each source will be observed three times for 5min within one observing block - therefore the LST range is given by the minimum overlap of the LST ranges of the individual sources in one block.

### Receivers requested:

We ask for L-band receivers in order to cover the HI, OH and radio recombination lines (RRLs), as well as the continuum.

**Samplers and correlator setup:**

We choose the correlator setup to include the HI 21 cm line, the four OH hyper-fine structure transitions and additional RRLs, as well as the continuum in full polarization:

- Given the large velocity range of HI emission in the Galactic plane, especially for sources towards the Galactic Center ( $>200$  km/s), we choose a bandwidth of HI of  $\sim 800$  km/s (4 MHz). This will also provide the sufficient range of emission-free channels necessary for the continuum subtraction. For the OH and RRLs we choose the band width accordingly.
- Many of the target regions show strong OH maser emission at their systemic velocity. While targeting a velocity resolution of 0.2 km/s, since maser features can be very narrow, we choose a channel width of  $\sim 0.1$  km/s (0.5 kHz) to avoid Gibbs ringing that would affect absorption signals at the velocities of clouds along the line of sight. For consistency, we choose the same channel width for HI, which allows us to resolve typical HI absorption lines in the cold neutral phase of the ISM. We will degrade the velocity in post-processing to increase sensitivity if necessary.
- For OH, we choose 1 band each for the transitions at 1612 MHz and 1720 MHz, and combine the 1665 and 1667 MHz transitions in one band with double band width.
- We propose to observe multiple RRLs between 1-2 GHz to increase the signal-to-noise in the final images by stacking them in velocity.
- For RRLs, we choose a velocity resolution of  $<1$  km/s (3.91 kHz), which is more than sufficient to resolve the hydrogen RRLs (typical line widths of  $\sim 25$  km/s), but still small enough to investigate narrow carbon RRL emission.
- We choose 8 bands to cover the full continuum between 1-2 GHz in full polarization.

**Frequency averaging factor:**

N/A

**Mosaic requirements:**

N/A

**Sensitivity:**

With 60min integration per pointing, we reach an RMS noise of  $\sim 8$  mJy/beam after smoothing to a velocity resolution of 0.2 km/s and of up to  $\sim 6$  mJy/beam at 0.4 km/s resolution (for HI the sensitivity may be slightly lower due to the contribution of HI emission to the system temperature).

For measuring HI and OH in absorption, the final RMS will typically depend on the strength of the continuum source. The strength of most of the continuum source in our sample varies between 0.4-4 Jy/beam, with about one half of the sources being similar or stronger than 1 Jy/beam at 1.4 GHz. Assuming therefore a typical source strength of 1 Jy/beam, this results in a typical 1sigma RMS of OH optical depths of  $\tau \sim 0.008$  at 0.2 km/s,  $\tau \sim 0.006$  at 0.4 km/s. Additional sensitivity can be gained by further smoothing. This will allow us to probe weak absorption from diffuse OH gas along the line of sight ( $\tau < \sim 0.01-0.05$ ) for most sources, while still improving in sensitivity and velocity resolution for sources with a continuum weaker than 1 Jy/beam over currently available large-scale surveys such as the THOR survey (Beuther et al., 2016) at reasonable integration times.

**Integration time:**

We require an on-source time of 60 min to obtain a RMS noise of  $\sim 8$  mJy/beam at 0.2 km/s. For the 22 sources, this corresponds to a total on-source integration time of 22 h.

We group the sources into three blocks of close-by sources to facilitate gain calibration and scheduling. As some of the sources have extended continuum, to improve the uv-coverage, we split the 60min into shorter chunks of 15 min, and observe them at different hour angles. We distribute the 15min across each scheduling block, alternating between different sources, to maximize the uv-coverage for each source.

We estimate  $\sim 30$ s slewing time between scans ( $\sim 1$  min for "Hygal Sourcegroup 3", as the sources are farther apart). Complex gain calibration will be done every  $\sim 20$ min on a close-by gain calibrator for  $\sim 2$ min. An additional time of  $\sim 15$ min is needed for bandpass calibration on 3C286. We account for 10 min startup time per block.



In total, this adds up to scheduling blocks of 3.3h, 3.0h and 2.4h for "Hygal Sourcegroup" 1,2 and 3, respectively. Each scheduling block needs to be repeated 4 times to reach 60min on-source time. Therefore, we request a total of 34.8 h of observing time at L-band in C-configuration.

**Dump time:**

Using GOST we configured our correlator units with 10sec dump time. The total data rate is 34.4 MB/s, which is within well limits for standard observations. This corresponds to ~4.3 Tb raw data volume for all observations combined.

**Imaging considerations:**

Since all sources are strong continuum and/or maser sources, we will take into account dynamic range limitations when performing the imaging. We split the observations for each source in three short observations at different hour angles to maximize the uv-coverage to improve the imaging of extended emission.

**Polarimetric considerations:**

N/A

**RFI considerations:**

The VLA Pipeline does an excellent job in flagging the data for good calibration. As HI is in a protected band, we typically expect only little RFI in this band. For the OH lines, occasional RFI can occur, which will be identified with manual flagging. For the RRLs and the continuum observations, we will use automatic flagging algorithms such as RFLAG in CASA.

**Joint considerations:**

N/A

**Other:**

Data processing will be conducted at a dedicated computing cluster at MPIfR in Bonn, equipped with large memory, highly sufficient disk storage and fast I/O.

## SCIENTIFIC JUSTIFICATION

### 1. Introduction

#### 1.1 Characterizing the diffuse ISM with absorption line spectroscopy

The past decade has seen huge advances in our understanding of the diffuse interstellar medium, driven observationally by absorption line spectroscopy of atoms and small molecules performed at millimeter and submillimeter wavelengths towards background continuum sources. Diffuse molecular clouds play a crucial role in the lifecycle of the interstellar medium, representing transitional objects that are intermediate between the diffuse atomic medium and the dense molecular clouds that are the sites of star formation. They provide a simple laboratory in which we can study a variety of physical and chemical processes of broad applicability in astrophysics.

At submillimeter wavelengths, observations performed using *Herschel*/HIFI, APEX, and SOFIA/GREAT have allowed the ground-state rotational transitions of several interstellar hydrides to be observed for the first time at high spectral resolution: these comprise OH (e.g. Wiesemeyer et al. 2016), H<sub>2</sub>O (e.g. Flagey et al. 2013), OH<sup>+</sup>, H<sub>2</sub>O<sup>+</sup> (e.g. Wyrowski et al. 2010; Ossenkopf et al. 2010; Gerin et al. 2010a; Neufeld et al. 2010a), CH (e.g. Gerin et al. 2010b, Wiesemeyer et al. ), CH<sup>+</sup> (Falgarone et al. 2010), ArH<sup>+</sup> (Schilke et al. 2014), SH<sup>+</sup> (Menten et al. 2011), SH (Neufeld et al. 2012a, 2015), HF (Neufeld et al. 2010b; Sonnentrucker et al. 2010), H<sub>2</sub>Cl<sup>+</sup> (Lis et al. 2010; Neufeld et al. 2012b), and HCl<sup>+</sup> (de Luca et al. 2012.) At the same time, millimeter wave observations have characterized the abundances of heavier species in diffuse clouds along multiple sight-lines to mm-wave continuum sources: these include C<sub>2</sub>H (Gerin et al. 2011), HCO<sup>+</sup>, HCN, HNC (Godard et al. 2010), CS, SO, and H<sub>2</sub>S (Neufeld et al. 2015). Finally, ***previous absorption-line observations of the 21 cm HI line (Winkel et al. 2017)***, acquired with the Karl G. Jansky Very Large Array in our 3-hour program 11B-236, ***have proven essential to the interpretation of many of these molecular data obtained at shorter wavelengths.*** In particular, many of the molecular ions studied with *Herschel* originate in diffuse *atomic* clouds where the H<sub>2</sub> fraction is small. The determination of their *abundances* within such clouds, which provide key diagnostic probes as described below, relies on measurements of the HI column density. Thus, our previous 3-hour JVLA program has provided ***enormous leverage for the exploitation of molecular data obtained in tens of hours of Herschel time.***

#### 1.2 Molecular abundances as diagnostic probes in diffuse atomic clouds

Interpreted in the context of detailed astrochemical models for the ISM, the measured abundances of small molecules provide a wealth of information about the environment in which they are found. For example, the OH, OH<sup>+</sup>, H<sub>2</sub>O<sup>+</sup>, and ArH<sup>+</sup> molecules, which are formed in reaction sequences initiated by cosmic-rays, have been used to probe (1) the molecular fraction in diffuse atomic clouds; and (2) the cosmic-ray ionization rate (CRIR) and its variation within the Galaxy (Neufeld & Wolfire 2016, 2017).

Because oxygen and argon have ionization potentials higher than that of hydrogen, both atoms are primarily neutral in the cold neutral medium; thus, the formation of OH, OH<sup>+</sup>, H<sub>2</sub>O<sup>+</sup>, and ArH<sup>+</sup> is driven by cosmic-ray ionization (Gerin et al. 2010a; Neufeld et al. 2010a; Neufeld & Wolfire 2016; Wiesemeyer et al. 2016).

As shown in Figure 1, the formation of  $\text{OH}^+$  and  $\text{H}_2\text{O}^+$  occurs in a reaction sequence initiated by the cosmic-ray ionization of H (upper pathway) or  $\text{H}_2$  (lower pathway). In the case of  $\text{ArH}^+$ , the formation pathway begins with the cosmic-ray ionization of Ar to produce  $\text{Ar}^+$ , which quickly reacts with  $\text{H}_2$  to form  $\text{ArH}^+$ . From a detailed analysis of the available *Herschel* data on  $\text{OH}^+$ ,  $\text{H}_2\text{O}^+$ , and  $\text{ArH}^+$ , in combination with HI 21 cm measurements obtained with JVLA, Neufeld & Wolfire (2017) obtained an estimate of the cosmic-ray ionization rate (CRIR) within diffuse atomic clouds (i.e. clouds with a molecular fraction of a few percent or less).

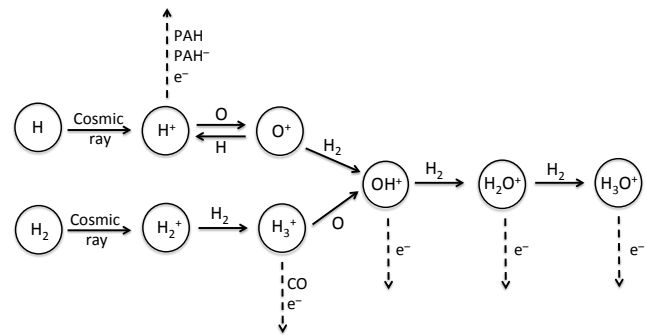


Figure 1: Chemical pathways leading to the oxygen hydride cations  $\text{OH}^+$ ,  $\text{H}_2\text{O}^+$  and  $\text{H}_3\text{O}^+$ . The dissociative recombinations of  $\text{H}_2\text{O}^+$  and  $\text{H}_3\text{O}^+$  lead to the formation of OH and  $\text{H}_2\text{O}$ . Dashed lines indicate competing reactions that reduce the abundance of these cations.

Figure 2 shows how observations of the  $N(\text{OH}^+)/N(\text{H})$  and  $N(\text{OH}^+)N(\text{H}_2\text{O}^+)$  column density ratios could be used to determine the CRIR within diffuse atomic clouds. Here, the  $N(\text{OH}^+)/N(\text{H})$  ratio is an increasing function of the CRIR, while the  $N(\text{OH}^+)/N(\text{H}_2\text{O}^+)$  ratio is an decreasing function of the  $\text{H}_2$  fraction,  $f(\text{H}_2)$ , and therefore the cloud size. The dependence of  $N(\text{OH}^+)/N(\text{H}_2\text{O}^+)$  on  $f(\text{H}_2)$  arises from the competition

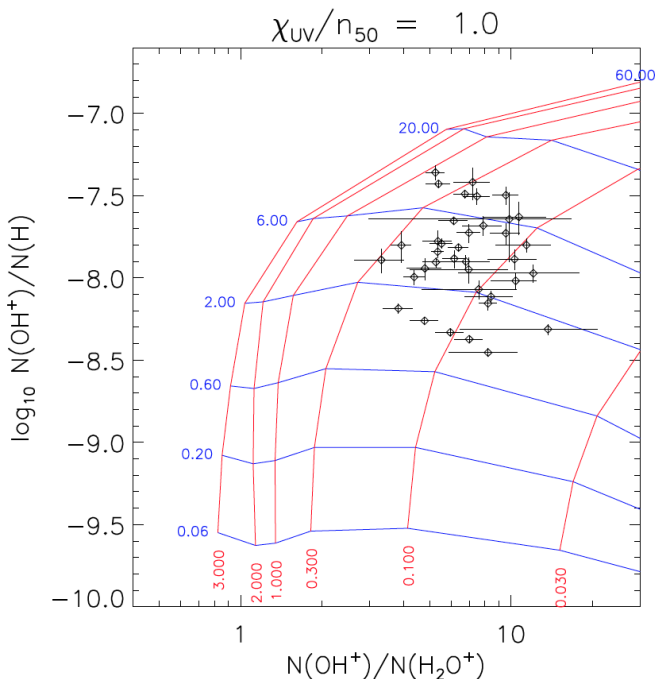


Figure 2:  $N(\text{OH}^+)/\text{H}$  and  $N(\text{H}_2\text{O}^+)/\text{OH}^+$  column density ratios observed toward 32 diffuse atomic clouds along the sight-lines to bright THz continuum sources. The red and blue curves show the prediction of a grid of models with different the cosmic ray ionization rates (blue values in units of  $10^{-16} \text{ s}^{-1}$ ) and total dust extinction (red values showing  $A_v$  in magnitudes)

between the dissociative recombination of  $\text{OH}^+$  to form O and the reaction with  $\text{H}_2$  to form  $\text{H}_2\text{O}^+$  (Figure 1). The average value obtained for the primary ionization rate per H atom,  $\zeta_p(\text{H}) = (2.2 \pm 0.3) \times 10^{-16} \text{ s}^{-1}$ , was in excellent agreement with entirely independent estimates of  $\zeta_p(\text{H})$  obtained for diffuse molecular clouds (with  $f(\text{H}_2) > 0.1$ ) from observations of  $\text{H}_3^+$ . This value, however, is an order of magnitude larger than (1) the typical cosmic-ray ionization rates inferred for dense molecular clouds and (2) expectations based on direct measurements of cosmic-rays obtained with the Voyager I spacecraft. This suggests (1) that cosmic-rays are excluded from dense molecular clouds (e.g. Padovani et al. 2009); and (2) that the cosmic-ray flux in the vicinity of the solar system may be atypical.

### 1.3 HyGAL: an approved SOFIA Legacy Program

Thus far, the absorption line observations described above have been performed toward relatively small sample of the brightest, most well-studied sources. Motivated by the advances thereby obtained, and with the goal of broadening the sample size and Galactic coverage obtained to date, we are carrying out a Joint (i.e. US - German) SOFIA Legacy Program, "HyGAL," over the next two years. ***This 82-hour program, which was approved in full last December, will conduct absorption line observations of six hydride molecules*** ( $\text{OH}^+$ ,  $\text{H}_2\text{O}^+$ ,  $\text{ArH}^+$ , SH, CH and OH) plus [OI] and [CII] toward twenty-five THz continuum sources in the Galactic plane. HyGAL will take advantage of the GREAT spectrometer to achieve the high resolution needed to spectrally resolve individual clouds along each sight-line. This program will greatly expand the sample of diffuse clouds that have been studied intensively through absorption line spectroscopy, providing significantly better coverage of the Galactic disk.

### 2. JVLA observations proposed here

***To fully exploit the data to be obtained in HyGAL, HI 21 cm observations are essential.*** Here, we propose to observe the 22 HyGAL sources lying within the JVLA declination range (Table 1). We will adopt a "maximum commensality" setup that allows simultaneous observations, with adequate spectral resolution, of the 1420 MHz HI line, all four 18 cm OH hyperfine transitions (1612, 1665, 1667, and 1720 MHz), and 18 radio recombination lines along with a significant stretch of continuum bandwidth. The observations will be performed in the C-array.

**Table 1:** Source list

Source	R.A. (J2000)	Decl. (J2000)	Source	R.A. (J2000)	Decl. (J2000)
W3 IRS 5	02h25m40.54s	+62°05'51.4"	G29.96 -0.02	18h46m03.72s	-02°39'21.2"
W3(OH)	02h27m04.10s	+61°52'22.1"	G31.41+0.3	18h47m34.10s	-01°12'49.0"
NGC 6334 I	17h20m53.35s	-35°47'01.5"	W43 MM1	18h47m47.00s	-01°54'28.0"
G357.558-00.321	17h40m57.19s	-31°10'59.3"	G32.80+0.19	18h50m30.62s	-00°02'00.0"
Sgr B2M	17h47m20.50s	-28°23'06.0"	G34.3+0.2	18h53m18.70s	+01°14'58.0"
HGAL0.55-0.85	17h50m14.52s	-28°54'30.7"	W49N	19h10m13.20s	+09°06'12.0"
G09.622+0.19	18h06m14.90s	-20°31'37.0"	G45.07+0.13	19h13m22.00s	+10°50'54.0"
G10.47+0.03	18h08m38.40s	-19°51'52.0"	W51	19h23m43.90s	+14°30'31.0"
G10.62-0.39	18h10m28.70s	-19°55'50.0"	DR21	20h39m01.60s	+42°19'37.9"
W33A	18h14m39.40s	-17°52'00.0"	DR21(OH)	20h39m00.70s	+42°22'47.0"
G19.61-0.23	18h27m38.00s	-11°56'39.5"	NGC 7538 IRS 1	23h13m45.31s	+61°28'11.7"

#### Our observations have two main goals:

First, our HI observations, together with single dish data, will yield HI column densities using the Lazareff (1975) method; as described in Section 1.2 above, these provide critical information for all chemical modeling efforts.

Second, the JVLA observations of OH absorption will provide a unique and valuable dataset for which 2.5 THz submillimeter ground-state rotational transition will also be observed with SOFIA. Because any interpretation of the 18 cm line strengths, which usually are not in thermal equilibrium, depends

critically on the excitation temperatures that are assumed for the various hyperfine states, ***the combination of JVLA and SOFIA data will provide a critical calibration of the 18 cm lines***. Technically speaking, the SOFIA observations of the 2.5 THz OH ground state line will deliver accurate values for the total OH column density that will provide a tight constraint for modeling the populations in the different hyperfine/lambda-doubling states within the lowest rotational state of OH. New calculations can now benefit from recently calculated collisional rate coefficients (Kłos et al. 2020). Such synergetic studies give hope that a straightforward interpretation of the 18 cm OH lines will be possible more than 55 years after their detection. Given the importance of such multiwavelength data, we will also include 8 additional sources for which previous SOFIA observations of the OH 2.5 THz line have already been performed.

## 2.1 Time Request

To detect HI and OH absorption from diffuse molecular gas along the line of sight to the targeted continuum sources, we propose for deep observations with an on-source time of 60 minutes for all sources in our sample, which adds up to 22 hours total on-source time.

With a final velocity resolution of 0.2 km/s, we expect to reach a rms noise of  $\sim 8$  mJy/beam (adding RCP and LCP). The continuum source strengths vary mostly between 0.4 – 4 Jy/beam, with half of the sources being similar or stronger than 1 Jy/beam at 21 cm. Assuming therefore an exemplary source strength of 1 Jy/beam, this will yield a  $1\sigma$  sensitivity in optical depth of  $\tau \sim 0.008$ . Since the sensitivity will be better than that for about half of the targeted sample, it will be possible to detect even weak optically-thin (intervening spiral arm) absorption components in HI, and weak and narrow OH absorption components from diffuse clouds with typical optical depths of  $\tau_{\text{peak}} \sim 0.01 - 0.05$  and lower (e.g., Li et al., 2018). For continuum sources which are weaker than 1 Jy/beam, this allows us to obtain OH and HI absorption spectra at much-improved sensitivity and velocity resolution over currently available large-scale surveys such as the THOR survey (Beuther et al., 2016) at reasonable integration times. In addition, we require time for careful, deep bandpass calibration and absolute flux calibration (on 3C286) and phase calibration on nearby phase calibrators. Our total time request is 34.8 hours.

## References

- Bialy, S., et al. 2017, ApJ, 843, 92  
Beuther, H., et al. 2016, A&A, 595, A32  
De Luca, M., et al., ApJ, 751, L37  
Falgarone et al. 2010, A&A 521 L15  
Flagey, N., et al. 2013, ApJ, 762, 11  
Gerin, M., et al. 2010a, A&A, 518, L110  
Gerin, M., et al. 2010b, A&A, 518, L16  
Godard, B., et al. 2009, A&A, 495, 847  
Godard, B., et al. 2012, A&A, 540, A87  
Godard, B., et al. 2014, A&A 570 A27  
Grenier, I., et al. 2005, Science 307, 1292  
Indriolo, N., et al. 2015, ApJ, 800, 40  
Kłos, J. et al. 2020, MNRAS, 493, 3491  
Lazareff, 1975, A&A, 42, 25  
Li, D., 2018, ApJS, 235, 1  
Menten, K. M., et al. 2011, A&A, 525, A77  
Neufeld, D. A., et al. 2010a, A&A, 521, L10  
Neufeld, D. A., et al. 2010b, A&A, 518, L108  
Neufeld, D. A., et al. 2012a, A&A, 521, L6  
Neufeld, D. A., et al. 2012b, A&A, 748, A37  
Neufeld, D. A., et al. 2015, A&A, 577, A49  
Neufeld, D. A., & Wolfire, M. G. 2016  
Neufeld, D. A., & Wolfire, M. G. 2017  
Ossenkopf, V. et al. 2010, A&A, 518, L111  
Padovani, M., et al. 2009, ApJ, 501, 619  
Schilke, P., et al. 2014, A&A, 566, A29  
Sheffer, Y., et al. 2008, ApJ, 687, 1075  
Sonnentrucker et al. 2015, ApJ, 806, 49  
Wiesemeyer et al. 2016, A&A, 585, 76  
Wiesemeyer et al. 2018, A&A, 612, 37  
Winkel, B., et al. 2017, A&A, 600, A2  
Wyrowski, F., et al. 2010, A&A, 518, A26

<b>Array Configuration</b>	C
<b>Number of Antennas</b>	25
<b>Polarization Setup</b>	Dual
<b>Type of Image Weighting</b>	Robust
<b>Representative Frequency</b>	1.4000 GHz
<b>Receiver Band</b>	L
<b>Approximate Beam Size</b>	14.94"
<b>Digital Samplers</b>	8 bit
<b>Elevation</b>	Medium (25°-50°)
<b>Average Weather</b>	Summer
<b>Calculation Type</b>	Noise/Tb
<b>Time on Source</b>	1h 0m 0s
<b>Total Time</b>	1h 15m 40s
<b>Frequency Bandwidth</b>	933.9795 Hz
<b>Line Velocity Width</b>	0.2000 km/s
<b>RMS Noise (units/beam)</b>	7.9430 mJy
<b>RMS Brightness (temp)</b>	22.1939 K
<b>RMS H I Column Density</b>	8.09190E+18
<b>Confusion Level</b>	7.1955 $\mu$ Jy

Produced by the NRAO EVLA Exposure Calculator v21A for semester 21A.